

Numerical Investigation on Heat Transfer Enhancement due to Assisting and Opposing Mixed Convection in an Open Ended Cavity

Antonio Carozza, Oronzio Manca, and Sergio Nardini

Abstract---Combined natural convection and forced convection gets a great attention for its importance in practical applications in various modern systems. Channels with an open cavity are of interest in electronic cooling, nuclear reactors, building management and solar energy systems. In these geometrical configurations, sometimes natural convection is insufficient for thermal management and control of such systems, so forced convection is required. Numerical investigation on mixed convection heat transfer in a two-dimensional channel with open cavity is investigated in this article. Forced flow assisting and opposing the motion generated by the natural convection inside the cavity is considered. A uniform temperature is considered to be associated alternatively on the left surface and on the right side of the cavity. The other surfaces are taken to be adiabatic. Governing equations are solved using the cell centered finite volume method commercial code Fluent. The simulation is carried out for a wide range of Reynolds numbers ($Re = 10-1000$) and Richardson numbers ($Ri = 0.1-1.7 \times 10^4$). Results are presented in the form of streamlines, average temperatures of the fluid, vertical velocities at mid-length of the channel and mean velocity fields. The conclusion is that the enhancement of heat transfer rate is generated principally by the increasing Re and the opposing configuration is thermally more efficient with respect to the assisting one.

Keywords---Mixed convection, opposing, assisting, open cavity, heat transfer enhancement, Nusselt number.

Nomenclature

$Re = HU_0/\nu$ Reynolds number
 $Gr = g\beta(T-T_0)D^3/\nu^2$ Grashoff number
 $Ri = Gr/Re^2$ Richardson number
 $Nu = hD/k$ Nusselt number
 L length of the cavity
 D height of the cavity
 U_i reference velocity
 U non dimensional velocity
 V non dimensional velocity
 u x velocity
 v y velocity
 X x coordinate
 Y y coordinate
 $Pr = \nu/\alpha$
 T_h hot wall temperature
 T_c cold wall temperature
 T_w wall temperature

Antonio Carozza, Fluid Dynamics Department, CIRA, Italian Aerospace Research Centre, Via Maiorise

Oronzio Manca, and Sergio Nardini, Industrial and Information Engineering Department, DIIE, Second University of Naples, Aversa, via Roma 29.

Greek Symbols

ν cinematic viscosity
 ρ density
 μ dynamic viscosity
 θ non dimensional temperature
 κ conductivity
 α thermal diffusivity
 Φ generic field variable

Subscripts

∞ free stream
 h hot
 c cold
 w wall
 o reference

I. INTRODUCTION

THE problem of mixed convection resulting from the flow over a cavity is of considerable theoretical and practical interest. Mixed convection in a heated cavity has many practical applications in various fields of engineering such as electronic components cooling, solar components or nuclear reactors. Nevertheless the only natural convection is not sufficient in some cases for the thermal control of such systems, so forced convection is used. Several studies are carried out on this matter, each one with a focus on a specific aspect of the possible variables to investigate:

1. Different cavities' shapes
2. Lid driven cavity/channel cavity
3. Different CFD methodologies

In the following table 1 a meaningful summary of the produced works on the matter is reported. Papanicolaou et al. [1] have conducted a computational analysis of mixed convection in turbulent regime in a channel with a cavity heated from one side. Two typical values of the Reynolds number are chosen, $Re=10^2$ and $Re=2.0 \times 10^3$, and turbulent results are obtained in the range $Gr=5 \times 10^7-5 \times 10^8$. For both values of Re , the average Nusselt number over the surface of the source is found to vary with Gr in a fashion consistent with previous numerical and experimental results for closed cavities, while the effect of Re in the chosen range of values is small. A numerical interesting study on mixed convection heat transfer in a ventilated cavity is also carried out by Papanicolaou et al. [2]. They studied in unsteady manner an isolated constant source of heat input within the enclosure for various parameters like Reynolds and aspect ratios and considering conductive walls. Oscillatory results characterized by a single frequency

were observed. Mahapatra et al. [3] have instead performed a numerical analysis for opposing mixed convection resulting due to wall movement and buoyancy induced by a clockwise fluid motion in a differentially heated cavity. The effect of Prandtl number (Pr) and wall surface emissivity (ϵ) has been investigated for different values of Richardson number. The effect of Prandtl number with respect to the transformation of a multi-cellular structure of streamline into a unicellular structure has been analyzed. For the same Richardson number (Ri) with an increase in Prandtl number, the flow and heat transfer phenomena changes from a buoyancy-induced dominated flow to a shear-induced dominated flow, which leads to some exciting results with respect to wall movement as well. Furthermore, the role of surface radiation in this respect has been emphasized. Islam Et al. [4] have performed a numerical study has been performed on mixed convection inside an open cavity on the bottom of a channel. One of the three walls of the cavity experiences a uniform heat flux while the other walls and the top of the channel are adiabatic. Three different cases are considered by applying uniform heat flux on (a) the inflow side (assisting forced flow); (b) the outflow side (opposing forced flow); (c) the bottom horizontal surface (transverse flow). For higher Richardson number, a better thermal performance is achieved for the transverse flow case. Aminossadati et al. [5] have numerically investigated mixed convection heat transfer in a two-dimensional horizontal channel with an open cavity. A discrete heat source is considered to be located on one of the walls of the cavity. Three different heating modes are considered which relate to the location of the heat source on three different walls (left, right and bottom) of the cavity. The analysis is carried out for a range of Richardson numbers and cavity aspect ratios. The results show that there are noticeable differences among the three heating modes. Manca et al. [6] have performed a mixed convection in an open cavity with a heated wall bounded by a horizontally insulated plate is studied numerically. Three basic heating modes are considered: (a) the heated wall is on the inflow side (assisting flow); (b) the heated wall is on the outflow side (opposing flow); and (c) the heated wall is the horizontal surface of the cavity (heating from below). Mixed convection fluid flow and heat transfer within the cavity is governed by the buoyancy parameter, Richardson number (Ri), and Reynolds number (Re). The maximum temperature values decrease as the Reynolds and the Richardson numbers increase. The effect of the $H=D$ ratio is found to play a significant role on streamline and isotherm patterns for different heating configurations. The opposing forced flow configuration has the highest thermal performance in terms of both maximum temperature and average Nusselt number. Islam et al. [7] have performed mixed convection in an open cavity with a heated wall bounded by a horizontally unheated plate is investigated experimentally. The cavity has the heated wall on the inflow side. Mixed convection fluid flow and

heat transfer within the cavity is governed by the buoyancy parameter, Richardson number (Ri), and Reynolds number (Re). The results show that the maximum dimensional temperature rise values decrease as the Reynolds and the Richardson numbers decrease. The flow visualization points out that for $Re = 10^2$ there are two nearly distinct fluid motions: a parallel forced flow in the channel and a recirculation flow inside the cavity. For $Re = 10^2$ the effect of a stronger buoyancy determines a penetration of thermal plume from the heated plate wall into the upper channel. Nusselt numbers increase when L/D increase in the considered range of Richardson numbers. Manca et al. [8] have also studied the mixed convection in an open cavity with a heated wall bounded by a horizontal unheated plate is investigated experimentally for a range of Reynolds numbers (Re) from 10^2 to 2.0×10^3 and Richardson numbers (Ri) from 4.3 to 6.4×10^3 . Also, the ratio between the length and the height of cavity (L/D) ranges from 0.5–2.0, and the ratio between the channel and cavity height (H/D) is equal to 1.0. At the lowest investigated Reynolds number, the surface temperatures are lower than the corresponding surface temperatures, for $Re = 2.0 \times 10^3$ at the same ohmic heat flux. For $Re = 10^3$ there are two nearly distinct fluid motions: a parallel forced flow in the channel and a recirculation flow inside the cavity. For $Re = 10^2$, the effect of a stronger buoyancy determines a penetration of thermal plumes from the heated plate wall into the upper channel. At higher Reynolds numbers, the vortex structure has a larger extension while L/D is held constant. A lack of research seems to be related to a numerical investigation on mixed convection in a ventilated cavity with forced flow opposing or assisting the natural convection in order to establish what is the best combination of the two convective modes. Several Reynolds and Grashoff are considered. A fixed aspect ratio L/D and variable Reynolds and Richardson numbers are considered for this simulation. A vertical wall of the cavity is at uniform temperature, the other vertical wall is at the inflow air temperature and the horizontal lower wall is adiabatic. A two-dimensional steady state regime is present in the analysis. Fields of stream function and temperature are reported while velocity profiles in several sections of the cavity and average Nusselt numbers are presented.

II. PHYSICAL MODEL-GOVERNING EQUATIONS

The geometry under investigation is shown in figure 1. Flow is laminar, incompressible and two-dimensional with negligible viscous dissipation. All the thermo-physical properties of the fluid are imposed constant except for the density varying with temperature following the Boussinesq approximation to take into account the buoyancy forces.

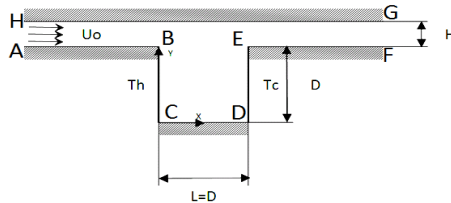


Fig. 1 Geometrical configuration under investigation

Considering the aforementioned assumptions, the governing equations can be written in non-dimensional form, as follows:

$$\frac{\partial U}{\partial X} + \frac{\partial V}{\partial Y} = 0 \tag{1}$$

$$U \frac{\partial U}{\partial X} + V \frac{\partial U}{\partial Y} = -\frac{\partial P}{\partial X} + \frac{1}{Re} \left(\frac{\partial^2 U}{\partial X^2} + \frac{\partial^2 U}{\partial Y^2} \right) \tag{2}$$

$$U \frac{\partial V}{\partial X} + V \frac{\partial V}{\partial Y} = -\frac{\partial P}{\partial Y} + \frac{1}{Re} \left(\frac{\partial^2 V}{\partial X^2} + \frac{\partial^2 V}{\partial Y^2} \right) + \frac{Gr}{Re^2} \theta \tag{3}$$

$$U \frac{\partial \theta}{\partial X} + V \frac{\partial \theta}{\partial Y} = \frac{1}{PrRe} \left(\frac{\partial^2 \theta}{\partial X^2} + \frac{\partial^2 \theta}{\partial Y^2} \right) \tag{4}$$

Where, $R = u_i / \nu$
 $Gr = g \beta_T (T_h - T_c) D^3 / \nu^2 \kappa$ $Pr = \nu / \alpha$

$Ri = Gr / Re^2$ are respectively the Reynolds number, the Grashoff number, Prandtl number and Richardson number. The above mentioned equations use the following non dimensional variables:

$$\left. \begin{aligned} X = \frac{x}{D} \quad Y = \frac{y}{D} = \frac{T - T_c}{T_h - T_c} \\ U = \frac{u}{u_i} \quad V = \frac{v}{u_i} \end{aligned} \right\} \tag{5}$$

The average Nusselt number is

$$Nu = \frac{1}{D} \int_0^D Nu(y) dy = \frac{1}{D} \int_0^D \frac{h(y)y}{\kappa} dy \tag{6}$$

With

$$h(y) = \frac{q}{T_w(y) - T_i} \tag{7}$$

Where, D is the height of the cavity and y is the vertical coordinate variable depending on the chosen reference system. The boundary conditions are set as shown in tables 2 and 3. The cavity has two walls on which uniform temperature is imposed, one hot and another one cold. Forced flow enters through the left inlet of the channel at a uniform velocity u_i and at ambient temperature. At the exit zero diffusion flux for

all variables (outflow boundary conditions) is considered.

TABLE I
BOUNDARY CONDITIONS FOR THE ASSISTING CONFIGURATION

Wall	u	v	T
ED	$u=0$	$v=0$	T_h
BC	$u=0$	$v=0$	T_c
AH	$u=u_o$	$v=0$	T_o
FG	$\partial u/\partial x=0$	$\partial v/\partial x=0$	$\partial T/\partial x=0$
CD,AB,EF,GH	$u=0$	$v=0$	$\partial T/\partial x=0$

TABLE II
BOUNDARY CONDITIONS FOR THE OPPOSING CONFIGURATION

Wall	u	v	T
ED	$u=0$	$v=0$	T_c
BC	$u=0$	$v=0$	T_h
AH	$u=u_o$	$v=0$	T_o
FG	$\partial u/\partial x=0$	$\partial v/\partial x=0$	$\partial T/\partial x=0$
CD,AB,EF,GH	$u=0$	$v=0$	$\partial T/\partial x=0$

III. NUMERICAL PROCEDURE

The numerical procedure used in this work is based on the projection methods and volume finite formulation. Computations were carried out using the commercial software FLUENT 6.1 [23] based on the finite volume method. Two channels were located upstream and downstream the U-shaped cavity, respectively. The upstream and downstream channels were 6D and 5D long, respectively. The segregated solution method was chosen to solve the governing equations, which were linearized implicitly with respect to the equation's dependent variables. The second-order upwind scheme was chosen for the unsteady energy and momentum equations. The Pressure Implicit with SIMPLE projection method chosen to couple pressure and velocity was the scheme used for the present simulation. The mesh size has been chosen so that a best compromise between running time and accuracy of the results may be found. The procedure has been based on grid refinement until the numerical results agree, within reasonable accuracy, with the analytical ones, obtained from the parallel flow approach developed in the next section. Preliminary tests were carried out to evaluate the effect of the grid dimension and of the extended domain. The grid mesh is structured in each case and optimized taking into account the grid adoption for $y+=1$ at adjacent wall region. The sketch of the chosen grid distribution is reported in Figure 2. A mesh size of 250 x250 nodes is good to represent the heat transfer in the cavity because any other refinement does not affect the results in appreciable manner. More details about the grid independence check are reported in table 3. The following convergence criterion is adopted to ensure the convergence of the dependent variables:

$$\frac{\Phi^{n+1} - \Phi^n}{\Phi^{n+1}} \leq 10^{-5} \tag{9}$$

Where Φ is the dependent variable and n is the iteration index. Variable grid sizes are considered in the present investigation to check the grid independency solutions.

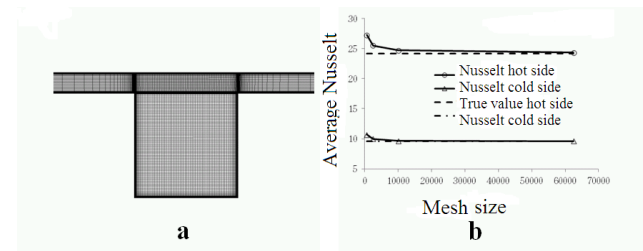


Fig. 2 Mesh detail, Nu –grid size diagram for grid independence analysis

TABLE III
GRID INDEPENDENCE CHECK

Reynolds	Grashoff	Mesh	Nusselt (hot wall)	error %	Nusselt (cold wall)	error %
10	2.70E+06	25x25	27.5	0.127049	10.5	0.036885
10	2.70E+06	50x50	25.1	0.028689	9.8	0.008197
10	2.70E+06	100x100	24.7	0.012295	9.7	0.004098
10	2.70E+06	250x250	24.5	0.004098	9.65	0.002049

IV. DISCUSSION OF RESULTS

A thermal analysis is carried out considering $H/D = 0.1$ and $L/D = 1.0$, while the Reynolds and Richardson numbers range respectively are from 10 to 1000 and from 0.1 to 2.3. Both assisting and opposing forced flow are taken into consideration. The effect of the Reynolds number on thermal and flow fields is first investigated. In assisting configuration, for small Re values ($Re = 10$), in figure 4(a-d), more recirculating cells are concentrated at the upper and lower side of the inlet channel section. As Re increases, the recirculating smaller cells vanish and only a great cell fill the cavity as shown in Figs. 4 (a-d). The corresponding temperature fields can be seen in Figs. 4 (a-h). It is observed that the increase in Re reduces the thermal boundary layer thickness and this is possible, since at larger value of Re , the effect of gravitation force becomes negligible. For lower Reynolds number the thermal transport due to buoyancy forces is predominant. The forced effect of the channel flow is negligible and the buoyancy effect predominates on the other the isotherms are quite at all near the wall where the forced flow ends. Both in assisting and opposing configurations isotherms are guided by the natural convection and the buoyancy effects are predominant while at Re 1000 they are guided by the forced flow in figures 4-5 (a-h). Indeed the velocity assumes a trend typical of a recirculating cell. This can also be observed by stream function distributions in figures 4(a-d). In the opposing configuration, instead, at lower Re the isotherms are concentrated near the hot wall as it can be observed in Fig. 5f. The forced effect of the channel flow is annealed and the buoyancy effect predominates while the isotherms are quite at all near the wall where the forced flow ends. Then the Richardson effect can be investigated. In the assisting configuration, as Ri increases the number of cells present within the cavity increases. The isotherms are more concentrated near the walls because of the fluid motion is mainly due to the buoyancy force and the effect of forced convection is lower. The heat flux is higher near the walls just because the recirculating cells fill almost the whole cavity. The conductive component of the heat flux is predominant when compared to lower Reynolds and

higher Grashoff cases. Temperature and stream function fields related to the opposing configuration are shown in Fig. 5. The streamlines and isotherms, as Ri increases, present forced convection as the main transport mechanism and several small non uniform recirculating cells are detected inside the cavity. They are located near the upper and lower zone at the inlet shown in Fig. 5a. Due to the buoyancy effect, i.e. for $Ri = 1.0$ the number of recirculating cells increases as shown in Fig. 5f. While the increase in Richardson number the cells are nearer to the cold wall and the hot wall. This is due to the increase in buoyancy forces determining a greater suction in hot wall. Thermal field is governed by interaction between incoming cold fluid stream and the circulating vortex. It also depends on where the vortex is created inside the cavity. For $Ri = 2.3$, the zone with high temperature becomes thinner near the hot wall and the temperature distribution is more uniform in the remaining parts of the cavity. On the other hand, the temperature decreases near the hot wall as the value of Ri increases as shown in Figs. 5(a-d). It can be seen that isothermal lines are vertically parallel to each other and concentrated around the heated wall, which is similar to conduction-like distribution. The stream function field shows that at lower Reynolds number the flow motion inside the cavity is very slow and there are small cells inside the cavity in each configuration. If you look at the values for the Nusselt number and Reynolds number reported in figure 6 the opposing configuration is considerably more effective in heat exchange, which is not trivial, as Reynolds increases if Manca et al. [8] have shown for similar cases with heated walls. This may be substantially due to the channel flow that acts directly on the hot wall rather than on the convective motion inside the cavity. The values of average Nusselt number increase decrease as Re increases, which is expected. The heat fluxes have a greater weight at higher Ri showing that the forced flow, at higher Re , can pull part of the heat flux out from the cavity while for higher Ri the buoyancy weight is surely predominant. It is evident that the best condition to enhance the heat transfer

is related to greater Re where the forced flows are responsible of the aforementioned enhanced heat transfer.

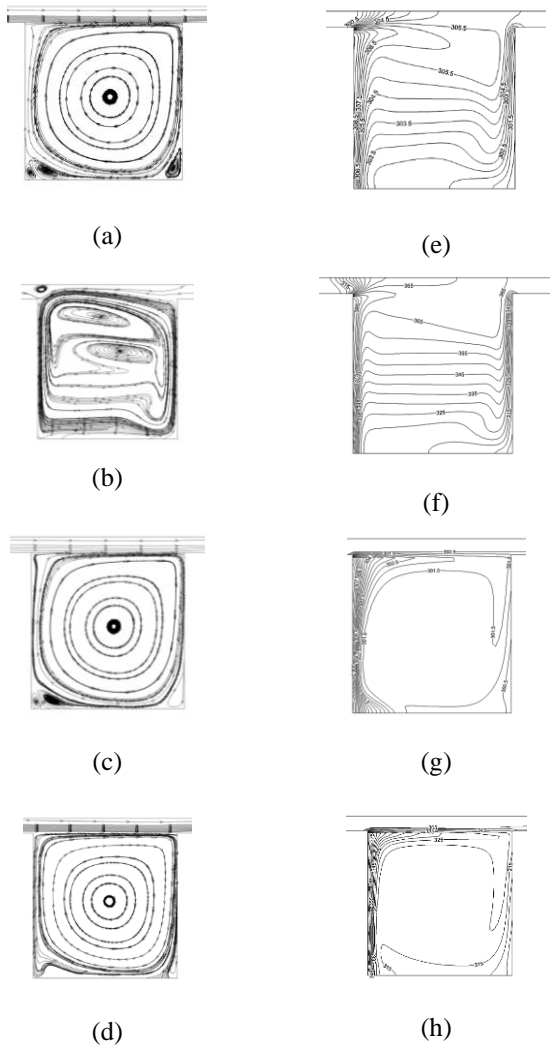


Fig. 4 Assisting flow configuration and: a) isotherms at Re=10 and Ri=1700; b) isotherms at Re=10 and Ri=17000; c) isotherms at Re=1000 and Ri=0.17; d) isotherms at Re=1000 and Ri=1.7; e) at Re=10 and Ri=1700; f) streamlines at Re=10 and Ri=17000; g) streamlines at Re=1000 and Ri=0.17; h) streamlines at Re=1000 and Ri=1.7.

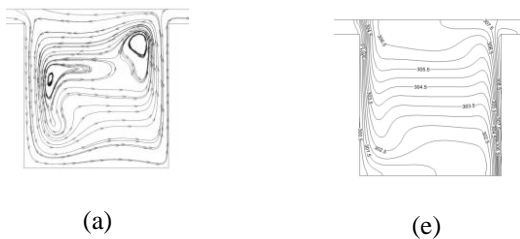


Fig. 5 Opposing flow configuration and: a) isotherms at Re=10 and Ri=1700; b) isotherms at Re=10 and Ri=17000; c) isotherms at Re=1000 and Ri=0.17; d) isotherms at Re=1000 and Ri=1.7; e) streamlines at Re=10 and Ri=1700; f) streamlines at Re=10 and Ri=17000; g) streamlines at Re=1000 and Ri=0.17; h) streamlines at Re=1000 and Ri=1.7.

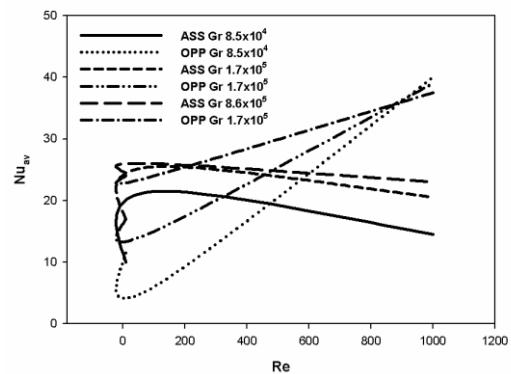


Fig. 6. Nu – Re diagrams

V. CONCLUSIONS

The present numerical investigation is performed on mixed convection in an enclosure with a forced flow coming from the channel located above. Results are obtained for different values of Re and Ri. A steady numerical analysis of mixed convection in a cavity located below a channel was accomplished. The cavity had two vertical walls at uniform temperature and the other surfaces unheated. Thermal and fluid dynamic behaviors of the case with the vertical heated wall of the cavity on the inlet forced flow side were evaluated for some Reynolds and Richardson numbers. The numerical investigation for two dimensional and laminar flow was carried out by means of the finite volume method

employing a commercial code. The results in terms of local Nusselt number, stream function and temperature fields. The following conclusions may be drawn from the present investigations

1. The average Nusselt number for an enclosure is significantly increased as Re is increased for both the flow configurations while the average temperature decreases.
2. The value of the average Nusselt number is greater for the opposing configuration with respect to the assisting configuration

This study can be applied in many industrial engineering fields such as in nuclear reactors in order to lower the temperatures or in the electronic systems in order to reduce the ventilation power useful and so the related costs. Possible further developments about this investigation are for example the use of different working fluids or aspect ratios involving eventually also an appropriate thermal optimization.

REFERENCES

- [1] E. Papanicolaou, Y. Jaluria, Mixed convection from a localized heat source in a cavity with conducting walls: a numerical study, Numerical heat transfer, Part. A, vol 23, pp. 463-484, 1993
<http://dx.doi.org/10.1080/10407789308913683>
- [2] E. Papanicolaou, Y. Jaluria, Computation of turbulent flow in mixed convection in a cavity with a localized heat source, Journal of heat transfer, august 1995, vol. 117, 649-658
<http://dx.doi.org/10.1115/1.2822626>
- [3] S.K. Mahapatra, S. Samantaray, and A. Sarkar, Role of Prandtl Number in the Interaction Phenomenon of Surface Radiation With an Opposing Mixed Convection Within a Differential Heated Cavity, Heat Transfer—Asian Research, 41 (4), 2012
- [4] Islam Mdt., Sumon Saha, Md. Arif Hasan Mamun and Mohammad Ali, Two Dimensional Numerical Simulation of Mixed Convection in a Rectangular Open Enclosure, FDMP, vol.4, no.2, pp.125-137, 2008
- [5] Oronzio Manca, Sergio Nardini & Kambiz Vafai, Experimental Investigation of Mixed Convection in a Channel With an Open Cavity, Experimental Heat Transfer, 19:53–68, 2006
<http://dx.doi.org/10.1080/08916150500318380>
- [6] Md. Tofiqul Islam, Sumon Saha, Md. Arif Hasan Mamun and Mohammad Ali, Two Dimensional Numerical Simulation of Mixed Convection in a Rectangular Open Enclosure, FDMP, vol.4, no.2, pp.125-137, 2008
- [7] S.M. Aminossadati, B. Ghasemi, A numerical study of mixed convection in a horizontal channel with a discrete heat source in an open cavity, European Journal of Mechanics Fluids 28 (2009) 590–598
<http://dx.doi.org/10.1016/j.euromechflu.2009.01.001>
- [8] Oronzio Manca, Sergio Nardini, Khalil Khanafer, Kambiz Vafai, Effect Of Heated Wall Position On Mixed Convection In A Channel With An Open Cavity, Numerical Heat Transfer, Part A, 43: 259–282, 2003
<http://dx.doi.org/10.1080/10407780307310>